NANO LETTERS

2001
Vol. 1, No. 4
183−187

Nanostructured Tungsten-Based Composite Coatings and Their Applications

Gregory M. Demyashev,* Alexander L. Taube, and Elias Siores

Industrial Research Institute Swinburne, Swinburne University of Technology, 533-545 Burwood Road, Hawthorn 3122, Melbourne, Australia

Received January 25, 2001

ABSTRACT

The object of the paper is the further investigation of unique superhard (35–40 GPa) nanocrystalline (nc) coatings based on W_3C phase, which is chemically vapor deposited at low temperature 400–700 °C and atmospheric pressure from the mixture of $WF_6 + C_3H_8 + H_2$ with the following partial pressure ratios: $WF_6/H_2 = 0.04–0.09$ and $C_3H_8/H_2 = 0.15–0.5$. Propane must be preliminarily subjected to catalytic cracking at 560–570 °C for 10–150 s in the presence of a stainless steel surface. The novel W_3C phase (A15 with $a_o = 0.5041$ nm) is different from well-known WC and W_2C by its associated lattice and Vickers microhardness ($HV_{0.5N}$) of 35–40 GPa. Deposits have shown that they are a mixture of both the W_3C phase and α- and β-carbynes, which are chainlike carbon structures $(–C≡C–)_n/(=C=C=)_n$. Nanocrystalline structure of the nc-W_3C/nc-carbyne composite with a nanocluster size of 2–100 nm, which is typical for the majority of novel superhard coatings, was discovered. It was shown that the nc-W_3C/nc-carbyne composite coatings have significant potential for industrial applications.

Materials with high hardness have always drawn attention. Conventionally, superhard materials[1] are defined as materials having hardness equal to or higher than 40 GPa. The current state of the art in superhard materials/coatings is summarized in Table 1, which includes the firmly fixed superhard materials/coatings with hardness higher than 40 GPa.[1−12] The tetrahedral amorphous (ta-C), or nonhydrogenated diamond-like carbon (DLC) mainly consisting of sp^3-bonded amorphous carbon (about 80%), superlattices {TiN/MeN (Me = Ta, TaW, Nb, V, Al, B), TiN/WC, and ZrN/CN_x}, and nanocomposites {nc-Me_nN/am-Si_3N_4 (Me = Ti, V, W), am-SiC/nc-SiC(β), and nc-TiAlN/nc-AlN} are qualified as superhard materials/coatings and have been synthesized recently. Natural diamond, boron carbide (B_4C), and cubic boron nitride (c-BN) are well known superhard materials.

Unfortunately, the others, such as hydrogenated DLC (a−C:H) and hypothetical carbon nitride (β-C_3N_4),[13,14] have shown relatively low hardness. Hydrogenated DLC, which has high hydrogen contamination (up to 50 at % of hydrogen),[4] and the carbon nitride exhibit only microhardness of 15−25 GPa and 20−30 GPa, respectively.

It is expected[15] that carbynes with the carbon-to-carbon triple/double bonds of sp^1 hybridization can be harder than B_4C. Carbynes are one-dimensional chainlike carbon structures $(-C≡C-)_n/(=C=C=)_n$,[16] as opposed to two-dimensional structure of graphite with sp^2-hybridization and three-dimensional structure of diamond with sp^3-hybridization.

Tungsten and tungsten carbides can significantly improve (or change[17]) some properties of DLC. Small addition of tungsten to ta-C results in a reduction of hardness from 72 to 63 GPa,[18] but that is accompanied by a corresponding remarkable decrease in intrinsic stress from 11 to 4.3 GPa. The formation of crystallites of WC_x carbide improves the temperature stability of the DLC up to 800 °C. Multilayer coatings being formed by alternating layers of fluorocarbon and β-WC_{1-x},[19] which has face-centered cubic NaCl-type structure, uniquely combine both the low frictional coefficient of 0.25 and microhardness of ∼35 GPa. It is generally accepted that two stable carbide phases in the W−C system are WC and W_2C.[20] Therefore, β-WC_{1-x} can be qualified as a new nonequilibrium phase.

CVD technologies offer the possibility to generate new nonequilibrium phases of tungsten carbide. It has been argued[21] that novel tungsten carbide coatings can be formed by CVD using a mixture of WF_6, C_3H_8, and H_2 at atmospheric pressure and low temperature. Krasovsky[22] has showed that a new tungsten carbide phase with microhardness of 35 GPa can be formed by varying the partial pressure ratio of propane to hydrogen. On the basis of chemical analysis and X-ray diffraction, the structure of the tungsten carbide CVD-deposited was identified as cubic structure of the A15 (Nb_3Sn type) with a lattice parameter $a_o = 0.5041$ nm. It is clear that there is still considerable interest in the W−C system and its further development as a promising source of superhard materials/coatings. The aim of the work

* Corresponding author: menglet@hotmail.com.

10.1021/nl015505h CCC: $20.00
Published on Web 03/24/2001

Table 1. Summary of Some Characteristics of Superhard Materials/Coatings

materials/coatings	crystal size[a] (nm)	hardness (GPa)	friction coefficient (.../against)	roughness (nm)	temp of stability (°C)
1. diamond	cr/pc/nc	70−100	0.1/steel	0.15−0.28	700
2. ta-C	am/nc	60−70	∼0.25/steel		300
3. B_4C (pc or nc)	0.1−100	40−70			1800
4. c-BN (pc or nc)	5−100	50−60			900
5. superlattices:					
TiN/MeN	5−10[b]	39−70			700
(Me = Ta, TaW, Nb, V, Al, B)					$1200_{TiN/AlN}$
TiN/WC	7	38−40			
ZrN/CN_x	1.6	∼40			
6. nanocomposites					
nc-Me_nN/am−Si_3N_4 (Me = Ti, V, W)	3−3.5	∼50			1100
am-SiC/nc-SiC(β)	am/nc	50/50			1600
nc-TiAlN/nc-AlN	30	40−47			

[a] ta − tetrahedral amorphous; am − amorphous; nc − nanocrystalline; cr − crystal; pc − polycrystalline. [b] Bilayer repeated period (Λ).

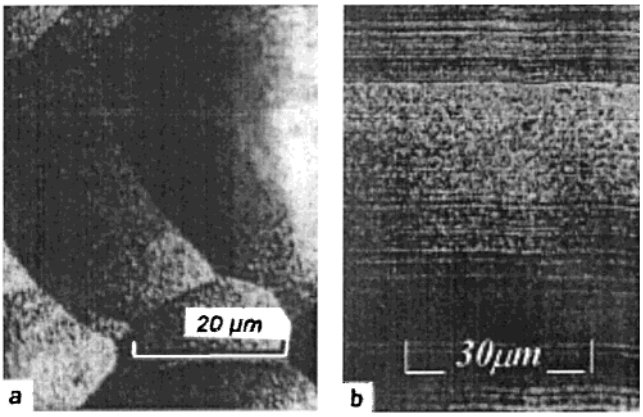

Figure 1. (a) Morphology of surface growth (scanning electron microscopy) and (b) lamellar microstructure of the cross-section (light microscopy).

was to further study of the novel tungsten carbide phase and assesses its potential industrial applications.

For the synthesis of the novel tungsten carbide,[22] the precursors WF_6, C_3H_8, and H_2 were fed into a hot wall furnace operated at atmospheric pressure and in the temperature range of 400−700 °C. It is important to note that these temperatures are much lower than conventional CVD, which is operated at around 1000 °C. Partial pressure ratios of precursors incorporated into the carrier gas (Ar) were as follows: WF_6:H_2 = 0.04−0.09 and C_3H_8:H_2 = 0.334−0.55. The flow rate of the mixture in a tube for the deposition was ∼12 cm s^{-1}. The tungsten carbide coatings produced were up to 300 μm in thickness. The deposition rate,[22] which can be varied by partial pressure of the precursors, can be in the range of 10−500 μm h^{-1}. Prior to deposition, propane was subjected to catalytic cracking over the stainless steel surface at 560−570 °C for 10−150 s. Catalytic cracking of the propane was found[21] to be essential in order to form the novel tungsten carbide coatings by chemical vapor deposition at low temperatures and atmospheric pressure.

The deposited tungsten carbide coatings, which usually have the globular surface morphology of the surface growth (Figure 1a) and a lamelliform structure of cross-section (Figure 1b), had been identified[22] with X-ray diffraction as the single-phase tungsten carbide deposits. The distance between lamellae can achieve up to 5 μm.

Table 2. Values of d_{hkl} Calculated from Electron Diffraction, X-ray Diffraction, and the Lattice Constant (a_o = 0.5041 nm) for W_3C

		calc	electron diffracton		X-ray diffraction
no.	*hkl*	d_{hkl} (nm)	d_{hkl} (nm)	I_{obsd}	d_{hkl} (nm)
1.			**0.5503**	15	
2.			**0.3820**	20	
3.			**0.2960**	10	
4.	200	0.2521	*0.2552*	75	0.2522
5.	210	0.2254	0.2282	80	0.2243
6.	211	0.2058	*0.2084*	100	0.2058
7.	220	0.1783	0.1724	10	0.1796
8.	222	0.1455	*0.1640*	10	0.1637
9.	320	0.1398	0.1470	45	0.1458
10.	321	0.1347	0.1424	10	0.1400
11.	400	0.1260	*0.1376*	70	0.1350
12.	420	0.1290	*0.1291*	25	0.1263
13.			**0.1254**	5	
14.			**0.1214**	5	
15.	421	0.1100	*0.1151*	5	0.1300
16.			**0.1118**	10	
17.	332	0.1075	0.1104	10	0.1104
18.	520		0.1050	5	0.1078
19.	521		0.0969	5	0.0930
20.	440	0.0892	0.0919	15	0.0919
21.			**0.0902**	5	
22.	660		0.0878	5	0.0894
23.			**0.0874**	5	
24.	610		0.0849	10	0.0841
25.	661	0.0818	0.0831	10	0.0829

Electron diffraction (ED) was used to resolve an exact phase composition of the deposits. First, the ED-results were in good accordance with known X-ray Diffraction and calculated data[22] (Table 2). The ED of the deposits revealed more about the structure and phases of the coatings. The ED-analysis indicated the presence of the additional diffraction rings (printed in bold in Table 2), unknown earlier, which exhibited low intensity (I_{obsd}) (Figure 2). Comparison

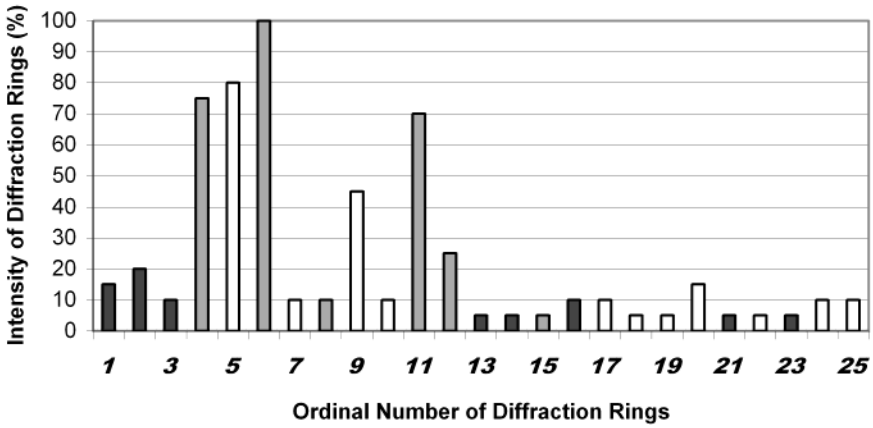

Figure 2. Schematic representation of the relative intensity of the electron diffraction rings: white, tungsten carbide (W_3C); black, carbynes with $(-C\equiv C-)_n$ and $(=C=C=)_n$; gray, possible overlapping the reflections of carbines and W_3C.

with the very well known carbon structures,[16,23] and carbides WC and W_2C,[20] showed that the extra electron diffraction rings belong to α- and β-carbynes and their mixture, chaoite. It is possible that the certain diffraction peaks printed in italic (Table 2) can overlap and represent both W_3C and α/β-carbynes.

Thus, the lamellar structure of the deposits was found to be bound up with co-deposition of the carbynes. The coatings are the composite of the two phases: one being the W_3C phase and the other α/β-carbynes. Owing to catalytic cracking, excess of propane in the gas mixture is dissociated, creating radicals. It is likely that the radicals result in the formation of sp^1 bonds.

The X-ray diffraction of the deposits had no sharp diffracting peaks. This provided a hint at the existence of very fine grain sizes of the deposits. Calculations from extended X-ray peaks[24] show the grain size to be an average of ~70 nm. Further direct TEM investigations using the dark- and bright fields of TEM images confirmed (Figure 3) that the composite deposits have first the nanocrystalline structure indeed, and second that they are the composite of nanoscale size of both the nc-W_3C phase and the nc-carbynes. The W_3C grains measuring in the range of 50−100 nm were in turn built of microclusters with size of 2−5 nm embedded within a very fine (up to 1 nm) carbyne matrix. Carbynes, which were present in the deposits throughout the volume of coatings, usually had size measuring between 2 and 5 nm.

The more detailed TEM study of the lamellar structure by layer-after-layer electron-microscopy analysis[25] showed that the carbyne content correlated with the alternation of the lamellae in deposits. Two kinds of the alternating layers were regularly formed in the composite deposits (Figure 4): on one hand, the layers with higher carbyne content, larger sizes of the carbyne crystallites (~5 nm), and smaller size of the W_3C clusters (up to 50 nm); on the other hand, the layers with lower carbyne content, smaller size of the carbyne crystallites (~2 nm), and bigger size of W_3C clusters (up to 100 nm).

Using the general correlation $D_{max} = 4R/3F$,[26] which can be applied for this case, where R is the radius of carbyne inclusions, F is their volumetric portion, and D_{max} is the maximum diameter of W_3C clusters for the given layer, it was possible to estimate the carbyne content in the lamella. The carbyne content of lamellar deposits varied from ~1 vol % to ~7 vol %, and the average percentage of carbynes in the deposit was found to be approximately 4 vol %.

Thus, the nanocrystallinity of the composite coatings, in conjunction with the unusual crystal structure of both the W_3C phase (A15-type lattice) and the carbynes (linear chainlike arrangement of carbon with double/triple bonds), was considered to be a major precondition of high hardness (~35 GPa) for the nc-W_3C/nc-carbyne coatings. The present results do not allow defining an obvious conclusion about any dominant cause of the hardness of these deposits. More work in this area is in progress.

More precise measurements of Vickers microhardness ($HV_{0.5N}$) of these coatings showed that microhardness is not constant and not equal to 35 GPa, as previously stated.[22] Repeated hardness measurements of cross-sections demonstrated the gradual alternation of the microhardness between 35 and 40 GPa that corresponds to the change of carbynes in lamellae.

The coefficient of friction was observed to be 0.12. It was tested with a pin-on-disk configuration over 10^5 cycles under a normal force of 10 N in air of 50% relative humidity. The M50-steel ball with 5 mm radius was used as the pin. Most probably, the addition of the carbynes in the composite coatings acts as a solid lubricant, which creates low frictional conditions. It is necessary to say that the layered Ti−TiC−TiC/DLC coatings,[27] which were then filled with MoS_2, exhibited the significantly lower friction coefficient of 0.02 in dry nitrogen atmosphere.

Investigation of the temperature stability of these coatings using an in situ heating system of TEM showed that the deposits decompose into tungsten, W_2C-carbide, and amorphous carbon at about 1200 °C. This temperature is significantly higher than 1000 °C, which was previously evaluated.[22]

As tested, the nc-W_3C/nc-carbyne compound coatings provide good anticorrosion functionality in H_2S, SO_2

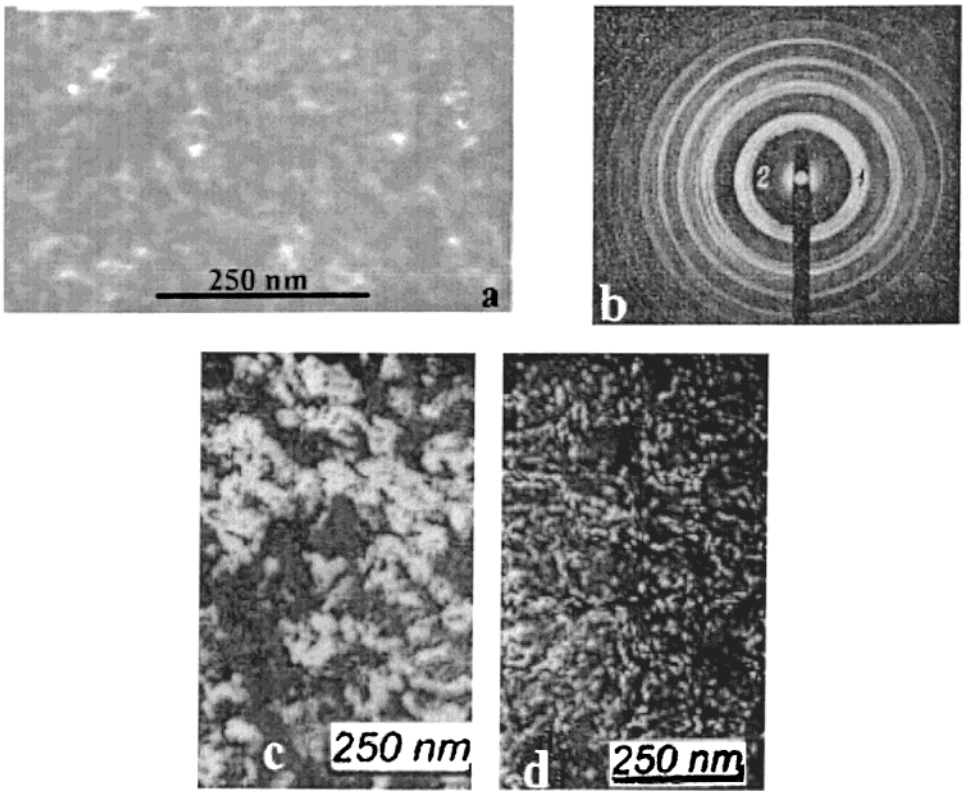

Figure 3. Typical transmission electron microscopy (TEM) images of the novel tungsten-based carbide phase: (a) bright field imaging; (b) selected-area diffraction pattern (1, dark field imaging (DFI) place for the electron diffraction rings ***4−5−6*** (see Figure 2), and 2, DFI place for the electron diffraction rings ***1−2−3*** (see Figure 2); (c) DFI of the selected electron diffraction rings ***4−5−6***; (d) DFI of the selected electron diffraction rings ***1−2−3***.

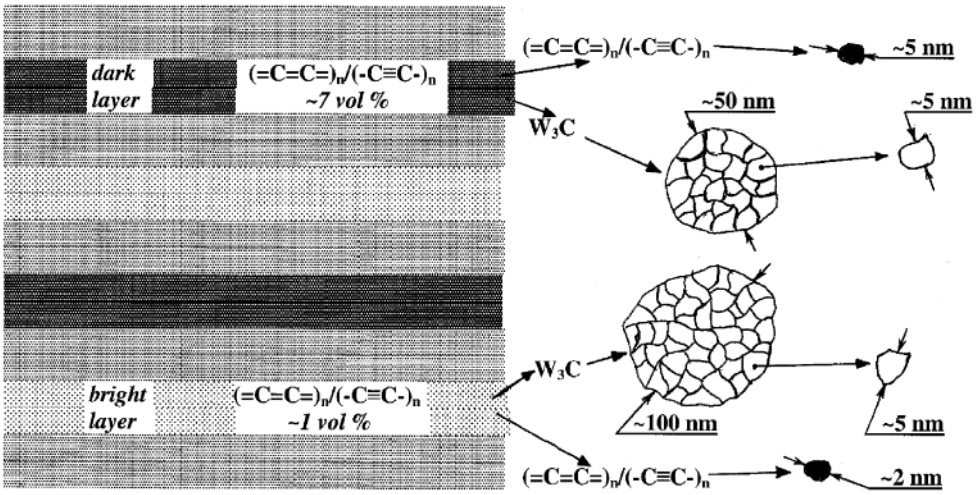

Figure 4. Illustration of the nanostructure of the nc-W_3C/nc-carbyne coatings.

(Kesternich DIN-50018 sulfur dioxide test), and other ambient aggressive conditions, owing to low coating porosity (less than 0.02%) and lack of through pinholes.

Customized properties of the coatings, such as friction and corrosion resistance, make the nanocomposite (nc-W_3C/nc-carbyne) very attractive in the manufacturing industry. These coatings can significantly prolong the lifetime and productivity of coated tools and parts. Certain diverse applications for engineering components, which were given a trial in industry recently and have shown good test data, are illustrated in Table 3.

For the first time in this research, the importance of carbynes and nanocrystalline microstructure of the composite nc-W_3C/nc-carbynes in chemically vapor-deposited coatings was recognized. The findings show that co-deposition of carbynes during crystallization of W_3C-coatings leads to the better tribological properties, such as low friction, wear, and corrosion resistance. This type of nanocomposite coating (nc-W_3C/nc-carbyne) permits blending of the important tribological properties that have traditionally been considered as mutually exclusive. In view of the results presented here, the nc-W_3C/nc-carbyne coatings, which are chemically

Table 3. Summary of Tool Wear-Life Improvement by nc-W_3C/nc-Carbyne Coating

tool substrate	improvement in wear life (times)
diamond, hard alloys and steel dies	2−7
Al-based extrusion dies	5−7
press and punching tools	2−3
cutting tools inserts	8−10
thread forming dies	8−12
moulds	3−7
sand and liquid jet nozzles	2−5
forming articles in civil engineering	10−12
oil-gas equipment	5−7
machine and automotive parts	7−10

Table 4. Summary of the Characteristics of Low-Thermal CVD Process and the nc-W_3C/nc-Carbyne Composite Coatings

precursor gas mixture	$W_6F + C_3H_8 + H_2$
deposition temperatures	400−700 °C
range of deposition rate	10−500 μm·h^{-1}
coating thickness	10−300 μm and more
microhardness	35−40 GPa
microstructure	nanocrystalline composite (nc-W_3C/nc−carbyne)
coating porosity	less than 0.02%
friction coefficient (coating/steel)	0.12 ± 0.02
friction coefficient (coating/coating)	0.1 ± 0.02
coating adhesion to HSS	up to 0.5 GPa
internal stress	0.5−1 GPa
W_3C lattice	A15 (a_o = 0.5041 nm)
density (nc-W_3C/nc−carbynes)	18.7 g/cm^3
gross carbon content	0.8 wt %
roughness	up to 1 μm
temperature stability	up to 1200 °C
fluorine contamination	≤0.3 at %

vapor-deposited, are an attractive supplement to the traditional superhard materials (Table 1). Table 4 summarizes some of the important performances of the low-thermal CVD processing and the nc-W_3C/nc-carbyne coatings. These nanocomposite coatings exhibit low internal stress, good adhesion, and high-temperature stability.

The present research extends the existing technologies[5,11] of synthesis of nanocomposite materials/coatings, which show the unexpected and potentially useful properties. This low-thermal chemical vapor deposition (LTCVD) introduces new possibilities in surface manufacturing processes and overcomes a number of disadvantages associated with conventional CVD. LTCVD eliminates the general shortcoming of conventional CVD, i.e., high processing temperature. The LTCVD can be carried out at 400−500 °C, which is comparable to plasma-assisted vapor deposition processes. LTCVD is also more versatile: it offers extra degrees of freedom to the chemical reactions and allows synthesizing the new (W_3C) or little-known (α/β-carbyne) phases with the nanoscale grain structure.

References

(1) Ulrich, S.; Theel T.; Schwan J.; Ehrhardt, H. *Surf. Coat. Technol.* **1997**, *97*, 45.
(2) Voevodin, A. A.; Donley, M. S.; Zabinski J. S. *Surf. Coat. Technol.* **1997**, *92*, 42.
(3) Barnett, S.; Madan, A. *Phys. World* **1998**, *1*, 45.
(4) Taube, K. *Surf. Coat. Technol.* **1998**, *98*, 976.
(5) Veprek, S. *Thin Solid Films* **1998**, *317*, 449.
(6) Wu, M.-L.; Qiana, W.-D.; Chunga, Y.-W.; Wangb, Y.-Y.; Wongb, M.-S.; Sproul, W. D. *Thin Solid Films* **1997**, *308−309*, 123.
(7) Selinder, T. I.; Sjöstrand, M. E.; Nordin, M.; Larsson, M.; Östlund, Å.; Hogmark, S. *Surf. Coat. Technol.* **1998**, *105*, 51.
(8) Veprek, S.; Nesládek, P.; Niederhofer, A.; Glatz, F.; Jílek, M.; Síma, M. *Surf. Coat. Technol.* **1998**, *108−109*, 138.
(9) Setoyama, M.; Irie, M.; Ohara, H.; Tsujioka, M.; Takeda, Y.; Nomura, T.; Kitagawa, N. *Thin Solid Films* **1999**, *341*, 126.
(10) Yoon, J. S.; Myung, H. S.; Han, J. G.; Musil, J. *Surf. Coat. Technol.* **2000**, *131*, 372.
(11) Musil, J.; Hrubý, H. *Thin Solid Films* **2000**, *365*, 104.
(12) Xu, J.-H.; Li, G.-Y.; Gu, M.-Y. *Thin Solid Films* **2000**, *370*, 45.
(13) Liu, A. Y.; Cohen, M. L. *Science* **1989**, *245*, 841.
(14) Chan, W.-C.; Zhou, B.-Z.; Chung, Y.-W.; Lee, C. S.; Lee, S. T. *J. Vac. Sci. Technol.* **1998**, *A16* (3), 1907.
(15) Whittaker, A. G. *U.S. Patent* No. 4,248,909.
(16) Heimann, R. B.; Keiman, J.; Salansky, N. M. *Carbon* **1984**, *22*, 147.
(17) Rusli, M.; Yoon, S. F.; Yang, H.; Ahn, J.; Huang, Q. F.; Zhang, Q.; Guo, Y. P.; Yang, C. Y.; Teo, E. J.; Wee, A. T. S.; Huan, A. C. H.; Watt, F. *Surf. Coat. Technol.* **2000**, *123*, 134.
(18) Monteiro, O. R.; Delplancke-Ogletree, M.-P., Lo, R. Yu.; Winand, R.; Brown, I. *Surf. Coat. Technol.* **1997**, *94/95*, 220.
(19) Costa, E.; Cavaleiro, A. *Surf. Coat. Technol.* **1997**, *97*, 680.
(20) Pierson, H. O. *Handbook of refractory carbides and nitrides*; Noyes Publications: Westwood, NJ, 1997.
(21) Krasovsky, A. I.; Sinani, I. L.; Kirillov, I. V.; Golovanov, Yu. N. USSR Patent No. 413,753. (Russ.)
(22) Krasovsky, A. I.; Chuzhko, R. K.; Tregulov, V. R.; Balachovsky, O. A. *Fluorine process of receipt of tungsten*; Nauka: Moscow, 1981; p 219. (Russ.)
(23) Pierson, H. O. *Handbook of carbon, graphite, diamond and fullerenes*; Noyes Publications: Westwood, NJ, 1993.
(24) Huber, C. A. In *Handbook of Nanophase Materials*; Marcel Dekker: NY-Basel-Hong Kong, 1997; p 317−336.
(25) Demyashev, G. M.; Chuzhko, R. K.; Repnikov, N. N.; Kislov, N. P. *Zavodskaya Laboratory* **1982**, *48*, p 61. (Russ.)
(26) Abrahamson, E. P. In *Ultra-fine Grain in Metals*; Pergamon Press: New York, 1973; p 82.
(27) Voevodin, A. A.; Bultman, J.; Zabinski, J. S. *Surf. Coat. Technol.* **1998**, *107*, 12.

NL015505H